crystals

MDPI

Article

Optical Properties of the Fresnoite $Ba_2TiSi_2O_8$ Single Crystal

Chuanying Shen [1,*], Huaijin Zhang [2], Duanliang Wang [2], Jiyang Wang [2] and Robert I. Boughton [3]

1 Shandong Provincial Key Laboratory of Laser Polarization and Information Technology, College of Physics and Engineering, Qufu Normal University, Qufu 273165, China
2 State Key Laboratory of Crystal Materials, Institute of Crystal Materials, Shandong University, Jinan 250100, China; huaijinzhang@sdu.edu.cn (H.Z.); wdliang012@163.com (D.W.); jywang@sdu.edu.cn (J.W.)
3 Department of Physics and Astronomy, Bowling Green State University, Bowling Green, OH 43403, USA; boughton@bgsu.edu
* Correspondence: shenshouchuan@163.com; Tel.: +86-537-5051-305

Academic Editor: Helmut Cölfen
Received: 1 January 2017; Accepted: 8 February 2017; Published: 11 February 2017

Abstract: In this work, using large-sized single crystals of high optical quality, the optical properties of $Ba_2TiSi_2O_8$ were systematically investigated, including transmission spectra, refractive indices and nonlinear absorption properties. The crystal exhibits a high transmittance (>84%) over a wide wavelength range from 340 to 2500 nm. The refractive indices in the range from 0.31256 to 1.01398 μm were measured, and Sellmeier's equations were fitted by the least squares method. The nonlinear absorption properties were studied by using the open-aperture Z-scan technique, with a nonlinear absorption coefficient measured to be on the order of 0.257 cm/GW at the peak power density of 16.4 GW/cm^2. Such high transmittance and wide transparency indicate that optical devices using the $Ba_2TiSi_2O_8$crystal can be applied over a wide wavelength range. Furthermore, the small nonlinear absorption observed in $Ba_2TiSi_2O_8$ will effectively increase the optical conversion efficiency, decreasing the generation of laser damage of the optical device.

Keywords: transmission spectra; refractive index; nonlinear absorption; Z-scan

1. Introduction

Fresnoite $Ba_2TiSi_2O_8$ (BTS) is tetragonal and belongs to the space group P4bm. The structure of BTS is characterized by TiO_5 square pyramids, which are the source of the strong spontaneous polarization in this crystal [1,2]. Benefiting from its polarizability, the BTS crystal exhibits excellent piezoelectric properties with large piezoelectric coefficients and electromechanical coupling factors [3,4], as well as high thermal stability up to the melting point of about 1445 °C. This behavior is in contrast to the homologous compound $Ba_2TiGe_2O_8$, which exhibits two phase transitions at −50 °C and 850 °C, respectively [5–8]. Therefore, BTS has been considered to be a good candidate for applications for surface acoustic wave, ultrasonic and sensor devices that can be used at high temperatures.

In addition to the piezoelectric properties, nonlinear optical, electro-optical, and elastic-optical properties as well as UV luminescence in BTS have been investigated. Takahashi found that BTS exhibits very large second-order optical nonlinearities (d_{33} = 13 ± 2 pm/V), comparable to those of $LiNbO_3$, and has potential applications in the fabrication of optical devices which can be used to generate frequency doubling in laser systems [9]. Based on its second-order optical nonlinearity, another feature of the BTS crystal is the electro-optic effect. Haussühl reported that BTS possesses a large electro-optical coefficient, which is of the same order of magnitude as that of KH_2PO_4, and so BTS is highly desirable for fabricating devices such as high-speed electro-optic modulators, optical shutters, and laser Q-switches which are used in the fields of laser modulation, optical communications

and optoelectronics [10–14]. Furthermore, BTS has proved to be a novel stimulated Raman scattering active crystal, where the Raman gain is slightly greater than that of $Ba(NO_3)_2$, and hence the crystal is suitable for solid-state Raman laser applications [15].

For the practical applications of frequency doubling, electro-optic and solid-state Raman laser devices, optical absorption can be induced by laser radiation. In particular, the existence of nonlinear absorption may decrease the frequency conversion efficiency, and may even result in internal damage when optical devices are used in a high-power laser system. Therefore, a better understanding of optical properties of crystalline material [16–18], especially the nonlinear absorption properties of the BTS crystal, is essential to realize its optical applications.

To our best knowledge, however, little attention has been paid to the nonlinear absorption properties of BTS crystals [19]. Studies reporting on the transmittance and refractive indices in BTS over a series of wavelength ranges are also very scarce, except for data at limited specific wavelengths [10,20,21]. All of these data are very important for the design and application of BTS optical devices. In this work, using large-sized single crystals of high optical quality grown by the Czochralski method, the optical properties of $Ba_2TiSi_2O_8$, including transmission spectra, refractive indices and nonlinear absorption properties, were systematically investigated. The transmittance and refractive indices were measured over a broad wavelength range, and the nonlinear absorption coefficients were studied by using the open-aperture Z-scan technique. These measurements were carried out for the purpose of obtaining a complete data set on the optical properties of BTS for future use in the design of optical applications.

2. Experimental Details

Large-sized $Ba_2TiSi_2O_8$ single crystals with high optical quality were successfully grown from the melt at 1445 °C by the Czochralski method [15,22]. The transmission spectrum, which reflects the linear transmittance and absorbance of the BTS crystal at different wavelengths of light, was measured by an IR-VIS-UV spectrophotometer (Hitachi U-3500, Jasco), using two polished *X*-cut and *Z*-cut square wafers with dimensions of $4 \times 4 \times 1$ mm^3. One finely polished prism was used to measure the refractive index by using a high precision measuring instrument (UV VIS SWIR IR 3-12, Trioptics, Germany).

The nonlinear absorption parameters of the BTS crystal were investigated by the open-aperture Z-scan technique, using polished *Z*-cut plates with dimensions of $8 \times 8 \times 2$ mm^3. A schematic diagram of the Z-scan technique is shown in Figure 1. A mode-locked Nd:YAG laser with a wavelength of 1064 nm and a repetition rate of 10 Hz was applied as the laser source. The nonlinear optical parameters were investigated in detail at the second harmonic generation (SHG) wavelength of 532 nm, where the pulse width and the focal length of the lens were about 30 ps and 30 cm, respectively. The average power could be directly controlled by using an optical attenuator. The basis of the Z-scan mechanism is that a focused Gaussian light beam is usually applied and approximately equally split into two beams by a beam splitter (BS). One beam is applied as a reference beam, while the other is used as the incident light beam to monitor the fluctuation of the laser density. The laser beam is focused by an objective lens. The incident laser peak power density gradually varies as the specimen moves nearer to the focal point of the lens [23]. The detectors D1 and D2 were used to measure the nominal optical power and the actual optical power, respectively. Thus, the normalized transmittance D2/D1 at different real-time position of BTS specimen could be simultaneously collected by a computer, which was collected to detectors D1 and D2.

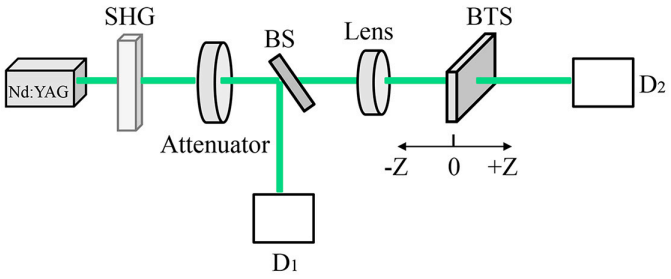

Figure 1. The schematic diagram of Z-scan technique.

Under the irradiation of a high power laser, the absorption coefficient cannot be ignored and is determined according to the following formula:

$$\alpha(\mathrm{I}) = \alpha + \beta \mathrm{I} \tag{1}$$

where α and β are the linear and nonlinear absorption coefficients, respectively, and I is the instantaneous intensity of the laser pulse. When the specimen moves along the $\pm Z$ direction, the normalized light transmittance T can be calculated using the following formula [24,25]:

$$T(z, s = 1) = \frac{\int_{-\infty}^{+\infty} \ln\left[1 + q_0(z,0)e^{-(t/\tau_p)^2}\right] d(t/\tau_p)}{\sqrt{\pi} q_0(z,0)} \tag{2}$$

Based on the two following Equations (3) and (4), the normalized light transmittance T can be reduced to a summation form more suitable for numerical evaluation [26]:

$$\int_{-\infty}^{\infty} \mathrm{e}^{-\mathrm{a}^2\mathrm{x}^2} \mathrm{dx} = \frac{\sqrt{\pi}}{\mathrm{a}} \tag{3}$$

$$\ln(1-\mathrm{x}) = -(\mathrm{x} + \frac{x^2}{2} + \frac{x^3}{3} + \frac{x^4}{4} + \ldots + \frac{x^n}{n}) = -\sum_{n=1}^{\infty} \frac{x^n}{n},\ \mathrm{n} \in \mathrm{N},\ -1 \le \mathrm{x} \le 1 \tag{4}$$

$$\begin{aligned} T(z, s = 1) &= \frac{\int_{-\infty}^{+\infty} - \sum_{n=1}^{\infty} \frac{[-q_0(z,0)\cdot e^{-(t/\tau_p)^2}]^n}{n} d(t/\tau_p)}{\sqrt{\pi}\cdot q_0(z,0)} \\ &= -\sum_{n=1}^{\infty} \frac{[-q_0(z,0)]^n}{\sqrt{\pi}\cdot q_0(z,0)\cdot n} \cdot \frac{\sqrt{\pi}}{\sqrt{n}} \qquad , \mathrm{m} = (\mathrm{n}-1) \in \mathrm{N} \\ &= \sum_{m=0}^{\infty} \frac{[-q_0(z,0)]^m}{(m+1)^{3/2}} \end{aligned} \tag{5}$$

The quantity $q_0(z,t)$ and the corresponding value of β are calculated directly from the following equation [24,25]:

$$q_0(z,t) = \beta I_0(t) L_{eff} / (1 + \frac{z^2}{z_0^2}) \tag{6}$$

where $L_{eff} = \frac{1-e^{-\alpha l}}{\alpha}$, $z_0 = \frac{\pi\omega_0^2}{\lambda}$, ω_0 is the waist radius, λ is the laser wavelength, l is the thickness of the specimen, and s is the aperture size.

3. Results and Discussion

3.1. Transmission Spectrum

The transmission spectra of BTS at room temperature are given in Figure 2. Clearly, the divergence of the transmittance along the *X*- and *Y*-axes was very small. The short cutoff wavelength extends into the ultraviolet region and no apparent absorption peaks appear, which indicates that the

influence of anomalous dispersion can be ignored in subsequent measurements of the refractive index. The transmittance over the wide wavelength range of 340–2500 nm approached 84%. Such high transmittance and wide transparency indicate that BTS optical devices can be applied over a wide wavelength range. In addition, the absorption coefficient, which is related to the transmittance but is independent of the sample size and is plotted over the wavelength range of 340–2500 nm, is shown in the inset of Figure 2.

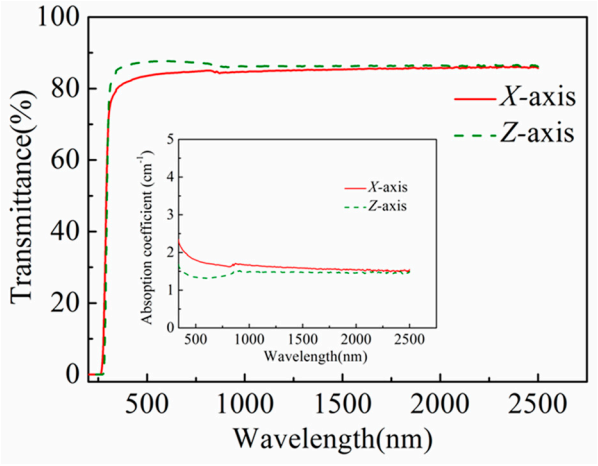

Figure 2. The transmission spectra of $Ba_2TiSi_2O_8$ at room temperature.

3.2. Refractive Index

$Ba_2TiSi_2O_8$ belongs to the tetragonal system, which is optically uniaxial and possesses only an ordinary refractive index (n_o) and an extraordinary refractive index (n_e). The refractive indices measured by the least deflection angle method with birefringence (Δn) are listed in Table 1, and the fitted dispersion curves in the wavelength range of 0.31256–1.01398 μm are presented in Figure 3.

Table 1. The refractive indices of BTS crystal measured at different wavelengths.

Wavelength (μm)	n_o	n_e	Δn
0.31256	1.86109	1.84596	0.01513
0.36502	1.82291	1.81381	0.00910
0.43584	1.79722	1.79166	0.00556
0.47999	1.78742	1.78304	0.00438
0.54608	1.78304	1.77736	0.00568
0.58756	1.77281	1.77008	0.00273
0.64385	1.76803	1.76582	0.00221
0.70652	1.76399	1.76223	0.00176
0.76819	1.76091	1.75949	0.00142
0.85211	1.75767	1.75664	0.00103
1.01398	1.75553	1.7430248	0.01251

From Table 1, BTS is found to be a negative uniaxial crystal ($n_o > n_e$) with a relatively small birefringence, where the refractive indices decrease with the increasing wavelength. The inset of Figure 3 shows a finely polished BTS prism used for the measurement of the refractive indices. The parameters of Sellmeier's equations that were fitted by the least squares method are listed in Table 2.

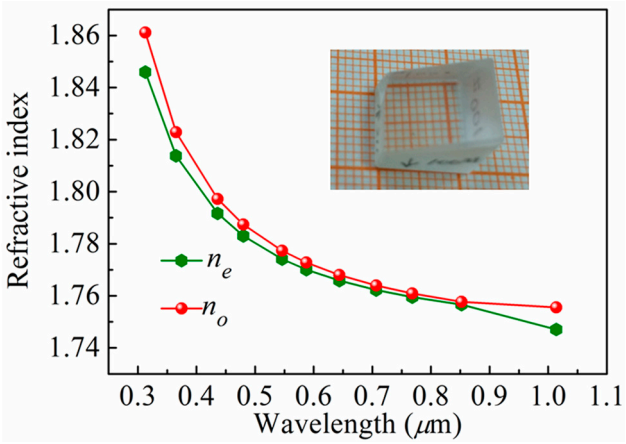

Figure 3. The measured refractive indices of $Ba_2TiSi_2O_8$ prism.

Table 2. The simulated parameters of Sellmeier's equations.

	A	B	C	D
n_o	3.0492 ± 0.0045	0.0294 ± 0.0010	0.0266 ± 0.0018	−0.013 ± 0.0045
n_e	3.1024 ± 0.0119	0.0183 ± 0.0023	0.0393 ± 0.0057	0.0734 ± 0.0128

Sellmeier's equations fitted by the least squares method can be expressed as:

$$n_o^2 = 3.0492 + \frac{0.0294}{\lambda^2 - 0.0266} + 0.0013\lambda^2 \quad (7)$$

$$n_e^2 = 3.1024 + \frac{0.0183}{\lambda^2 - 0.0393} - 0.0734\lambda^2 \quad (8)$$

Using a fit to Sellmeier's equations, the refractive indices of BTS at different wavelengths can be calculated, which is very important information to use in the design for optical applications. For example, the refractive indices at a wavelength of 0.40466 μm can be calculated and are found to be n_o = 1.8066, n_e = 1.7993. These values are in good agreement with the measured values of n_o = 1.8065, n_e = 1.7998.

3.3. Z-Scan Performance

Figure 4 illustrates the normalized transmittance curves of BTS, where the dotted lines represent the experimental data, and the solid lines correspond to the theoretical results fitted to Equation (5). The "valley" characteristic especially clearly demonstrates the existence of nonlinear absorption, and the "valley" depth indicates its magnitude. Furthermore, from Reference [27] and our experimental data, the fitting curves are in good agreement with two-photon absorption but not with three-photon absorption. So, most likely, the nonlinear absorption in our experiment is due to the former.

From an analysis of the fitting data, we obtained the corresponding value of $q_0(z,t)$. The nonlinear absorption coefficient β was then calculated using Equation (6) and the data was found to be 0.257 cm/GW. Referring to Table 3 and other literature sources, the nonlinear absorption coefficient of BTS was seen to be smaller than those of commercialized optical crystals, such as $KTiOPO_4$ (25 cm/GW) [28], $LiNbO_3$ (0.56 cm/GW) [29], and carboxylic acid–doped KH_2PO_4 (11.4–89.9 cm/GW) [30]. Small nonlinear absorption will effectively increase optical conversion efficiency and decrease laser damage when the crystal is applied as an optical device.

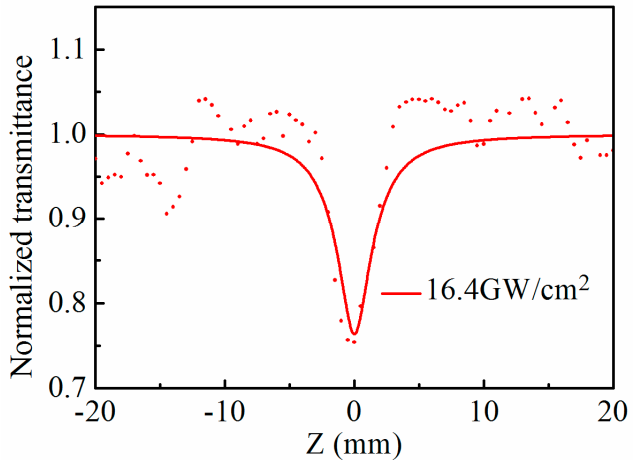

Figure 4. Normalized transmittance as a function of distance Z.

Table 3. The nonlinear optical parameters of BTS crystal at λ = 532 nm.

Peak Power Density (GW/cm^2)	Nonlinear Optical Parameters	
	β (cm/GW)	$\chi_I^{(3)}$ (10^{-13}esu)
16.4	0.257 ± 0.019	5.46 ± 0.4

The nonlinear susceptibility reflects the strength of the interaction between an optical field and the material. The imaginary part of the nonlinear susceptibility $\chi_I^{(3)}$ is associated with nonlinear absorption [31], and can be calculated using Equation (9) [32,33]. Under pico-second or femto-second laser irradiation, when the value of the nonlinear susceptibility $\chi^{(3)}$(esu) is on the order of 10^{-12}~10^{-14}, nonlinear absorption is mainly associated with distortion of the electron cloud and with the molecular orientation [26]. The $Ba_2TiSi_2O_8$ crystals are in the solid state rather than the liquid state, so there likely is no molecular orientation effect. In this experiment, the magnitude of $\chi_I^{(3)}$(esu) was about 10^{-13}, so we hypothesized that the nonlinear absorption of BTS is most likely related to electron cloud distortion [26,34].

$$\chi_I^{(3)}(esu) = \frac{c^2 {n_0}^2 \beta}{240\pi^2\omega}(m/W) \quad (9)$$

where c is the velocity of light in a vacuum, n_0 is the linear refraction index, and ω is the optical frequency.

4. Conclusions

In summary, the optical properties, including the transmission spectrum, refractive indices and nonlinear absorption properties, of the $Ba_2TiSi_2O_8$ crystal were systematically investigated. The transmittance was measured to be 84% over the wide wavelength range of 340–2500 nm. The refractive indices were studied by using the least deflection angle method, and were determined to decrease as the wavelength increased from 0.31256 to 1.01398 μm, as obtained by fitting to Sellmeier's equations using the least squares method. The nonlinear absorption is mainly associated with distortion of the electron cloud in $Ba_2TiSi_2O_8$. The nonlinear absorption coefficient was calculated to be 0.257 cm/GW at the peak power density of 16.4 GW/cm^2. High transmittance and a wide transparency range contribute to the excellent prospect of optical device applications utilizing BTS crystals over a wide wavelength range. Furthermore, the small nonlinear absorption in $Ba_2TiSi_2O_8$ will effectively increase the optical conversion efficiency and decrease the generation of laser damage in optical devices.

Acknowledgments: This work is supported by National Natural Science Foundation of China (Grant No. 51602174) and the Natural Science Foundation of Shandong Province (No. ZR2016EMQ04).

Author Contributions: Chuanying Shen contributed in the preparation, characterization, and analysis of transmission spectrum and refractive indices of the material, and wrote the paper; Huaijin Zhang conceived and designed the experiments, contributed in ideological guidance and equipment support; Jiyang Wang contributed in the discussion of experimental results, analysis of data and revision of the paper. Duanliang Wang contributed in the characterization and analysis of nonlinear optical experiment (Z-scan) part; Robert I. Boughton contributed in revision of the paper both for English and physics.

Conflicts of Interest: The authors declare no conflict of interest.

References

1. Moore, P.B.; Louisnathan, S.J. Fresnoite: Unusal Titanium Coordination. *Science* **1967**, *156*, 1361–1362. [CrossRef] [PubMed]
2. Masai, H.; Tsuji, S.; Fujiwara, T.; Benino, Y.; Komatsu, T. Structure and non-linear optical properties of BaO-TiO_2-SiO_2 glass containing $Ba_2TiSi_2O_8$ crystal. *J. Non-Cryst. Solids* **2007**, *353*, 2258–2262. [CrossRef]
3. Kimura, M.; Fujino, Y.; Kawamura, T. New piezoelectric crystal: Synthetic fresnoite ($Ba_2Si_2TiO_8$). *Appl. Phys. Lett.* **1976**, *29*, 227–228. [CrossRef]
4. Shen, C.-Y.; Zhang, H.-J.; Cong, H.-J.; Yu, H.-H.; Wang, J.-Y.; Zhang, S.-J. Investigations on the thermal and piezoelectric properties of fresnoite $Ba_2TiSi_2O_8$ single crystals. *J. Appl. Phys.* **2014**, *116*, 044106. [CrossRef]
5. Halliyal, A.; Bhalla, A.S.; Cross, L.E. Phase transitions, dielectric, piezoelectric and pyroelectric properties of barium titanium germanate $Ba_2TiGe_2O_8$ single crystals. *Ferroelectrics* **1985**, *62*, 3–9. [CrossRef]
6. Kimura, M.; Utsumi, K.; Nanamatsu, S. Ferroelastic behavior in $Ba_2Ge_2TiO_8$. *J. Appl. Phys.* **1976**, *47*, 2249–2251. [CrossRef]
7. Markgraf, S.A.; Bhalla, A.S. Low-temperature phase transition in $Ba_2TiGe_2O_8$. *Phase Transit.* **1989**, *18*, 55–76. [CrossRef]
8. Schmid, H.; Genequand, P.; Tippmann, H.; Pouilly, G.; Guedu, H. Pyroelectricity and related properties in the fresnoite pseudobinary system $Ba_2TiGe_2O_8$-$Ba_2TiSi_2O_8$. *J. Mater. Sci.* **1978**, *13*, 2257–2265. [CrossRef]
9. Takahashi, Y.; Benino, Y.; Fujiwara, T.; Komatsua, T. Large second-order optical nonlinearities of fresnoite-type crystals in transparent surface-crystallized glasses. *J. Appl. Phys.* **2004**, *95*, 3503–3508. [CrossRef]
10. Haussühl, S.; Eckstein, J.; Recker, K.; Wallrafen, F. Growth and physical properties of fresnoite $Ba_2TiSi_2O_8$. *J. Cryst. Growth* **1977**, *40*, 200–204. [CrossRef]
11. Yu, X.-Y.; Wang, H.-Y.; Rong, X.-W. Origin of the giant quadratic electro-optic effect in $KTa_{1-x}Nb_xO_3$ single crystals. *Opt. Mater.* **2015**, *46*, 429–431. [CrossRef]
12. Chang, Y.-C.; Wang, C.; Yin, S.-Z.; Hoffman, R.C.; Mott, A.G. Giant electro-optic effect in nanodisordered KTN crystals. *Opt. Lett.* **2013**, *38*, 4574–4577. [CrossRef] [PubMed]
13. Delre, E.; Mei, F.D.; Parravicini, J.; Parravicini, G.; Agranat, A.J.; Conti, C. Subwavelength anti-diffracting beams propagating over more than 1000 Rayleigh lengths. *Nat. Photonicst* **2015**, *9*, 228–232.
14. Tian, H.; Yao, B.; Zhou, Z.X.; Wang, H.F. Voltage-controlled diffraction modulation in manganese-doped potassium sodium tantalate niobate single crystals. *Appl. Phys. Express* **2012**, *5*, 012602. [CrossRef]
15. Shen, C.-Y.; Wang, D.-L.; Zhang, H.-J.; Wang, J.-Y.; Boughton, R.-I. Fresnoite $Ba_2TiSi_2O_8$—A novel stimulated Raman scattering active crystal. *Appl. Phys. Express* **2016**, *9*, 122402. [CrossRef]
16. Tian, H.; Zhou, Z.; Gong, D.; Wang, H.; Liu, D.; Jiang, Y. Growth and optical properties of paraelectric $K_{1-y}NayTa_{1-x}Nb_xO_3$ single crystals. *Appl. Phys. B* **2008**, *91*, 75–78. [CrossRef]
17. Tian, H.; Hu, C.P.; Meng, X.D.; Tan, P.; Zhou, Z.X.; Li, J.; Yang, B. Top-Seeded Solution Growth and Properties of $K_{1-x}Na_xNbO_3$ Crystals. *Cryst. Growth Des.* **2015**, *15*, 1180–1185. [CrossRef]
18. Wang, X.-P.; Li, Q.-G.; Yang, Y.-G.; Zhang, Y.-Y.; Lv, X.-S.; Wei, L.; Liu, B.; Xu, J.-H.; Ma, L.; Wang, J.-Y. Optical, dielectric and ferroelectric properties of $KTa_{0.63}Nb_{0.37}O_3$ and Cu doped $KTa_{0.63}Nb_{0.37}O_3$ single crystals. *J. Mater. Sci. Mater. Electron.* **2016**, *27*, 13075–13079. [CrossRef]
19. Wisniewski, W.; Nagel, M.; Rüssel, C. Macroscopic, Glass-Permeated Single-Crystals of Fresnoite. *CrystEngComm* **2015**, *17*, 5019–5025. [CrossRef]
20. Robbins, C.R. Synthesis and growth of fresnoite ($Ba_2TiSi_2O_8$) from a TiO_2 flux and its relation to the system $BaTiO_3$-SiO_2. *J. Res. Natl. Bur. Stand. A Phys. Chem.* **1969**, *74*, 229–232. [CrossRef]

21. Bechthold, P.S.; Haussühl, S.; Michael, E.; Eckstein, J.; Recker, K.; Wallrafen, F. Second Harmonic Generation in Fresnoite, $Ba_2TiSi_2O_8$. *Phys. Lett.* **1978**, *65A*, 453–454. [CrossRef]
22. Shen, C.-Y.; Zhang, H.-J.; Cong, H.-J.; Yu, H.-H.; Wang, J.-Y.; Zhang, S.-J. Voltage-controlled diffraction modulation in manganese-doped potassium sodium tantalate niobate single crystals. *J. Appl. Phys.* **2014**, *116*, 044106. [CrossRef]
23. Seema, R.; Sandeep, C.S.S.; Philip, R.; Kalarikkal, N. An open aperture *Z*-scan study of Sr_2CeO_4 blue phosphor. *J. Alloys Compd.* **2011**, *509*, 8573–8576. [CrossRef]
24. Sheik-Bahae, M.; Said, A.A.; Wei, T.-H.; Hagan, D.J.; Van Stryland, E.W. Sensitive measurement of optical nonlinearities using a sinlge beam. *IEEE J. Quantum Electron.* **1990**, *26*, 760–769. [CrossRef]
25. Wei, R.F.; Tian, X.L.; Zhang, H.; Hu, Z.L.; He, X.; Chen, Z.; Chen, Q.Q.; Qiu, J.R. Facile synthesis of two-dimensional WS_2 with reverse saturable absorption and nonlinear refraction properties in the PMMA matrix. *J. Alloys Compd.* **2016**, *684*, 224–229. [CrossRef]
26. Hong, L.Y. The Investigations of the Third Order Nonlinear Optical Properties and Response Time of DMIT Type Materials. Doctoral Dissertation of Shandong University, Jinan, Shandong Province, China, 2006. (In Chinese)
27. Zhao, G.; Zhang, F.; Wu, Y.Z.; Hao, X.P.; Wang, Z.P.; Xu, X.G. One-Step Exfoliation and Hydroxylation of Boron Nitride Nanosheets with Enhanced Optical Limiting Performance. *Adv. Opt. Mater.* **2016**, *4*, 141–146. [CrossRef]
28. Maslov, V.A.; Mikhailov, V.A.; Shaunin, O.P.; Shcherbakov, I.A. Nonlinear absorption in KTP crystals. *Quantum Elect.* **1997**, *27*, 356–359. [CrossRef]
29. Badorreck, H.; Nolte, S.; Freytag, F.; Baune, P.; Dieckmann, V.; Imlau, M. Scanning nonlinear absorption in lithium niobate over the time regime of small polaron formation. *Opt. Mater. Express* **2015**, *5*, 2729–2741. [CrossRef]
30. Anis, M.; Muley, G.G.; Hakeem, A.; Shirsat, M.D.; Hussaini, S.S. Exploring the influence of carboxylic acids on nonlinear optical (NLO) and dielectric properties of KDP crystal for applications of NLO facilitated photonic devices. *Opt. Mater.* **2015**, *46*, 517–521. [CrossRef]
31. Zhong, J.S.; Zhao, H.J.; Zhang, C.L.; Ma, X.; Pei, L.; Liang, X.J.; Xiang, W.D. Sol–gel synthesis and optical properties of $CuGaS_2$ quantum dots embedded in sodium borosilicate glass. *J. Alloys Compd.* **2014**, *610*, 392–398. [CrossRef]
32. Zhang, C.L.; Xiang, W.D.; Luo, H.Y.; Liu, H.T.; Liang, X.J.; Ma, X.; Pei, L.; Chen, Z.P.; Li, J.S.; Gao, H.H.; Ma, L. Third-order optical nonlinearity of Na_2O-B_2O_3-SiO_2 glass doped with lead nanoparticles prepared by sol–gel method. *J. Alloys Compd.* **2014**, *602*, 221–227. [CrossRef]
33. Fan, H.L.; Wang, X.Q.; Ren, Q.; Li, T.B. Third-order nonlinear optical properties in $[(C_4H_9)_4N]_2[Cu(C_3S_5)_2]$-doped PMMA thin film using Z-scan technique in picosecond pulse. *Appl. Phys. A* **2010**, *99*, 279–284. [CrossRef]
34. Wang, D.L.; Li, T.B.; Wang, S.L.; Wang, J.Y.; Wang, Z.P.; Ding, J.X.; Li, W.D.; Shen, C.Y.; Liu, G.X.; Huang, P.P. Effect of Fe^{3+} on third-order optical nonlinearity of KDP single crystals. *CrystEngComm* **2016**, *18*, 9292–9298. [CrossRef]